

Eta absorption by mesons

W. Liu and C. M. Ko¹ and L. W. Chen²

¹*Cyclotron Institute and Physics Department,*

Texas A&M University, College Station, Texas 77843-3366

²*Institute of Theoretical Physics, Shanghai Jiao Tong University, Shanghai 200240, China*

Abstract

Using the $[SU(3)_L \times SU(3)_R]_{\text{global}} \times [SU(3)_V]_{\text{local}}$ chiral Lagrangian with hidden local symmetry, we evaluate the cross sections for the absorption of eta meson (η) by pion (π), rho (ρ), omega (ω), kaon (K), and kaon star (K^*) in the tree-level approximation. With empirical masses and coupling constants as well as reasonable values for the cutoff parameter in the form factors at interaction vertices, we find that most cross sections are less than 1 mb, except the reactions $\rho\eta \rightarrow K\bar{K}^*(\bar{K}K^*)$, $\omega\eta \rightarrow K\bar{K}^*(\bar{K}K^*)$, $K^*\eta \rightarrow \rho K$, and $K^*\eta \rightarrow \omega K$, which are a few mb, and the reactions $\pi\eta \rightarrow K\bar{K}$ and $K\eta \rightarrow \pi K$, which are more than 10 mb. Including these reactions in a kinetic model based on a schematic hydrodynamic description of relativistic heavy ion collisions, we find that the abundance of eta mesons likely reaches chemical equilibrium with other hadrons in nuclear collisions at the Relativistic Heavy Ion Collider.

PACS numbers: 25.75.Nq, 12.39.Fe, 13.75.Lb, 14.40.Aq

I. INTRODUCTION

Besides the intrinsic interest of studying eta meson production in heavy ion collisions [1], knowledge of the eta meson dynamics in the hot dense matter formed in these collisions is also important for understanding other observables measured in experiments. For example, to extract information on the rho meson in-medium properties from the dilepton spectrum it emits requires reliable knowledge on the number of eta mesons produced in heavy ion collisions as eta mesons through their Dalitz decays contribute significantly to low-mass dileptons measured in these collisions [2]. Also, the two-pion correlation function measured via the Hanbury-Brown-Twiss interferometry is affected by pions from eta decays [3]. Understanding the eta meson dynamics is thus essential for extracting the size of the pion emission source from the pion interferometry. In heavy ion collisions at energies available from the Heavy Ion Synchrotron (SIS) at the German Heavy Ion Research Center (GSI), whose dynamics is dominated by baryons, the final eta number is mainly determined by its interaction with the nucleon through the N(1535) resonance [4], which has a branching ratio of about 35% decaying into pion and nucleon. At higher energies from the Super Proton Synchrotron (SPS) at the European Organization for Nuclear Research (CERN), the matter becomes more dominated by mesons, and the eta-meson interaction is thus important in determining the final eta yield [5]. For heavy ion collisions at the Relativistic Heavy Ion Collider (RHIC) at Brookhaven National Laboratory (BNL), the final hadronic matter is largely made of mesons, and it is even more crucial to have a good knowledge on the cross sections for eta meson absorption by mesons.

Since there is no empirical information on these cross sections, theoretical models are needed to evaluate their values. A possible model is the $[SU(3)_L \times SU(3)_R]_{\text{global}} \times [SU(3)_V]_{\text{local}}$ chiral Lagrangian with hidden local symmetry [6]. This model has been used to study previously dilepton production [7] and more recently the interactions of phi mesons in hot hadronic matter [8]. In this paper, we shall use this model to evaluate the cross sections for the absorption of η meson by π meson to the final states of $K\bar{K}$, $K\bar{K}^*(\bar{K}K^*)$, $K^*\bar{K}^*$, $\rho\omega$, and $\pi\rho$; by ρ meson to the final states of $K\bar{K}$, $K\bar{K}^*(\bar{K}K^*)$, $K^*\bar{K}^*$, $\rho\rho$, $\pi\omega$, and $\pi\pi$; by ω meson to the final states of $K\bar{K}$, $K\bar{K}^*(\bar{K}K^*)$, $K^*\bar{K}^*$, and $\pi\rho$; and by K and K^* to the final states of $K(K^*)\pi$, $K(K^*)\rho$, and $K(K^*)\omega$. In evaluating the cross sections for these reactions, we do not include the effects due to scalar mesons $a(980)$ and $a(1450)$ as

studies based on the non-linear chiral Lagrangian have shown that contributions from these resonances are unimportant compared to those from the vector meson exchanges and contact interactions [9]. These cross sections are then used in a kinetic model to study their effects on eta meson abundance in heavy ion collisions at RHIC.

This paper is organized as follows. In Section II, we give a brief description of the $[SU(3)_L \times SU(3)_R]_{\text{global}} \times [SU(3)_V]_{\text{local}}$ chiral Lagrangian with hidden local symmetry. The interaction Lagrangians that are relevant for describing the absorption of η meson by π , ρ , ω , K , and K^* are derived in Section III. The cross sections for these reactions are then evaluated in Section IV. In Section V, the time evolution of η meson abundance in relativistic heavy ion collisions is studied in a schematic model. Finally, a summary is given in Section VI. Explicit expressions for the amplitudes for η meson absorption are given in Appendices A-E.

II. CHIRAL LAGRANGIAN WITH HIDDEN LOCAL SYMMETRY

Based on the hidden local gauge symmetry, Bando [6] has constructed an effective theory for hadrons interacting at low energies. In this approach, vector mesons are introduced as the gauge bosons of the hidden local symmetry of the nonlinear chiral Lagrangian. For hadrons in the SU(3) multiplets, which are relevant for present study, it is constructed with two SU(3)-matrix valued variables $\xi_L(x)$ and $\xi_R(x)$ that transform as $\xi_{L,R}(x) \rightarrow \xi'_{L,R}(x) = h(x)\xi_{L,R} g_{L,R}^\dagger$ under $h(x) \in [SU(3)_V]_{\text{local}}$ and $g_{L,R} \in [SU(3)_{L,R}]_{\text{global}}$. The resulting chirally invariant Lagrangian is

$$\mathcal{L} = \mathcal{L}_A + a\mathcal{L}_V - \frac{1}{2} \langle F_{\mu\nu} F^{\mu\nu} \rangle, \quad (1)$$

with

$$\begin{aligned} \mathcal{L}_A &= -\frac{1}{4}f_\pi^2 \langle (D_\mu \xi_L \cdot \xi_L^\dagger - D_\mu \xi_R \cdot \xi_R^\dagger)^2 \rangle, \\ \mathcal{L}_V &= -\frac{1}{4}f_\pi^2 \langle (D_\mu \xi_L \cdot \xi_L^\dagger + D_\mu \xi_R \cdot \xi_R^\dagger)^2 \rangle, \\ F_{\mu\nu} &= \partial_\mu V_\nu - \partial_\nu V_\mu - ig[V_\mu, V_\nu]. \end{aligned} \quad (2)$$

In the above, f_π is the pion decay constant, the symbol $\langle \cdot \rangle$ denotes the trace of 3×3 matrix, and $D_\mu = \partial_\mu - igV_\mu$ is the covariant derivative, with the dynamical gauge bosons V_μ of the

hidden local symmetry identified with the nonet of vector mesons, i.e.,

$$V_\mu = \frac{1}{\sqrt{2}} \begin{pmatrix} \frac{1}{\sqrt{2}}\rho_\mu^0 + \frac{1}{\sqrt{2}}\omega_\mu & \rho_\mu^+ & K_\mu^{*+} \\ \rho_\mu^- & -\frac{1}{\sqrt{2}}\rho_\mu^0 + \frac{1}{\sqrt{2}}\omega_\mu & K_\mu^{*0} \\ K_\mu^{*-} & \bar{K}_\mu^{*0} & \phi_\mu \end{pmatrix}. \quad (3)$$

The above effective Lagrangian with $a = 2$ is known to give the universality of vector meson coupling, the Kawarabayashi-Suzuki-Riazuddin-Fayyazuddin (KSUF) relations [10], and the vector meson dominance of the pseudoscalar meson electromagnetic form factor [11].

Fixing the $[SU(3)_V]_{\text{local}}$ gauge by

$$\xi_L^\dagger = \xi_R \equiv \xi = \exp(i\Phi/f_\pi), \quad (4)$$

where Φ is the nonet of pseudoscalar Goldstone bosons

$$\Phi = \frac{1}{\sqrt{2}} \begin{pmatrix} \frac{1}{\sqrt{2}}\pi^0 + \frac{1}{\sqrt{3}}\eta + \frac{1}{\sqrt{6}}\eta' & \pi^+ & K^+ \\ \pi^- & -\frac{1}{\sqrt{2}}\pi^0 + \frac{1}{\sqrt{3}}\eta + \frac{1}{\sqrt{6}}\eta' & K^0 \\ K^- & \bar{K}^0 & -\frac{1}{\sqrt{3}}\eta + \sqrt{\frac{2}{3}}\eta' \end{pmatrix}, \quad (5)$$

leads to the usual lowest-order chiral Lagrangian

$$\mathcal{L}_A = -\frac{f_\pi^2}{4} \langle (\partial_\mu \xi \cdot \xi^\dagger - \partial_\mu \xi^\dagger \cdot \xi)^2 \rangle = \frac{f_\pi^2}{4} \langle \partial_\mu U \partial^\mu U^\dagger \rangle, \quad (6)$$

with $U = \xi^2$. In obtaining Eq.(5), we have used the empirical mixing angle $\theta \approx -20^\circ$ [12, 13] between the octet η_8 and the singlet η_1 to obtain the physical η and η' via $\eta \approx (2\sqrt{2}\eta_8 + \eta_1)/3$ and $\eta' \approx (-\eta_8 + 2\sqrt{2}\eta_1)/3$.

The $SU(3)$ symmetry breaking effects are taken into account by introducing in the Lagrangian the mass term

$$\mathcal{L}_{SB} = \frac{1}{4} f_\pi^2 \langle \xi_L \mathcal{M} \xi_R^\dagger + \xi_R \mathcal{M} \xi_L^\dagger \rangle, \quad (7)$$

with the mass matrix \mathcal{M} given by

$$\mathcal{M} = \text{diag}(m_\pi^2, m_\pi^2, 2m_K^2 - m_\pi^2). \quad (8)$$

Also, \mathcal{L}_A and \mathcal{L}_V are modified as follows [14]:

$$\begin{aligned} \mathcal{L}_A + \Delta\mathcal{L}_A &= -\frac{1}{4} f_\pi^2 \langle (D_\mu \xi_L \cdot \xi_L^\dagger - D_\mu \xi_R \cdot \xi_R^\dagger)^2 (1 + \xi_L \epsilon_A \xi_R^\dagger + \xi_R \epsilon_A \xi_L^\dagger) \rangle, \\ \mathcal{L}_V + \Delta\mathcal{L}_V &= -\frac{1}{4} f_\pi^2 \langle (D_\mu \xi_L \cdot \xi_L^\dagger + D_\mu \xi_R \cdot \xi_R^\dagger)^2 (1 + \xi_L \epsilon_V \xi_R^\dagger + \xi_R \epsilon_V \xi_L^\dagger) \rangle, \end{aligned} \quad (9)$$

with $\epsilon_{A(V)} = \text{diag}(0, 0, c_{A(V)})$, where $c_{A(V)}$ are real parameters to be determined by empirical hadron masses and decay constants.

Expanding the pseudoscalar fields in the first equation of Eq.(9) shows that the kinetic terms for K and η are renormalized by the symmetry breaking term. The proper kinetic terms can be recovered by rescaling the K and η fields according to [14]

$$\sqrt{1+c_A}K \rightarrow K \quad \text{and} \quad \sqrt{1+\frac{2}{3}c_A}\eta \rightarrow \eta. \quad (10)$$

As a result, the kaon and eta decay constants are related to the pion decay constant by

$$f_K = \sqrt{1+c_A}f_\pi \quad \text{and} \quad f_\eta = \sqrt{1+\frac{2}{3}c_A}f_\pi, \quad (11)$$

and masses of vector mesons become different, i.e.,

$$m_\rho^2 = m_\omega^2 = \frac{m_{K^*}^2}{1+c_V} = \frac{m_\phi^2}{1+2c_V} = af_\pi^2 g^2. \quad (12)$$

Expanding the Lagrangian up to four meson fields leads to interaction Lagrangians of the VPP, VVV, VVPP, and PPPP types, i.e.,

$$\begin{aligned} \mathcal{L}_{VPP} &= -i\frac{a}{2}g \langle \{[\Phi, \partial_\mu \Phi], V^\mu\} (1+2\epsilon_V) \rangle, \\ \mathcal{L}_{VVV} &= ig \langle (\partial_\mu V_\nu - \partial_\nu V_\mu)[V^\mu, V^\nu] \rangle, \\ \mathcal{L}_{VVPP} &= -ag^2 \langle V_\mu V^\mu (\epsilon_V \Phi^2 + 2\Phi \epsilon_V \Phi + \Phi^2 \epsilon_V) \rangle, \\ \mathcal{L}_{PPPP} &= \frac{2}{3} \frac{1}{f_\pi^2} \langle \partial_\mu \Phi \Phi \partial^\mu \Phi \Phi - \partial_\mu \Phi \partial^\mu \Phi \Phi^2 \rangle + \frac{1}{3f_\pi^2} \langle \mathcal{M} \Phi^4 \rangle \\ &\quad - \frac{1}{f_\pi^2} \langle \partial_\mu \Phi \partial^\mu \Phi (2\Phi \epsilon_A \Phi + \Phi^2 \epsilon_A + \epsilon_A \Phi^2) \rangle. \end{aligned} \quad (13)$$

In the chiral Lagrangian with hidden local symmetry, vector mesons have also been included through the anomalous interaction of the VVP type in order to take into account the breaking of local chiral symmetry [15]. Including further the flavor breaking through a term $\xi_L \epsilon_{wz} \xi_R^\dagger + \xi_R \epsilon_{wz} \xi_L^\dagger$ with $\epsilon_{wz} = \text{diag}(0, 0, c_{wz})$ [14], the total anomalous interaction Lagrangian then reads as

$$\mathcal{L}_{VVP} + \Delta \mathcal{L}_{VVP} = 2g_{VVP} \epsilon^{\mu\nu\lambda\sigma} \langle \partial_\mu V_\nu (1+2\epsilon_{wz}) \partial_\lambda V_\sigma \Phi \rangle. \quad (14)$$

III. INTERACTION LAGRANGIANS

Inserting Eqs.(3) and (5) in Eqs.(13) and (14) and rescaling the K and η meson fields according to Eq.(10), we obtain following interaction Lagrangian densities that are relevant

to η meson absorption by π , ρ , ω , K , and K^* :

$$\begin{aligned}
\mathcal{L}_{\rho\pi\pi} &= \frac{ag}{2} \vec{\rho}^\mu \cdot (\vec{\pi} \times \partial_\mu \vec{\pi}), \\
\mathcal{L}_{\rho KK} &= i \frac{ag}{4} \frac{1}{1+c_A} (\bar{K} \vec{\tau} \partial_\mu K - \partial_\mu \bar{K} \vec{\tau} K) \cdot \vec{\rho}^\mu, \\
\mathcal{L}_{\omega KK} &= i \frac{ag}{4} \frac{1}{1+c_A} (\bar{K} \partial_\mu K - \partial_\mu \bar{K} K) \omega^\mu, \\
\mathcal{L}_{K^* K \pi} &= i \frac{ag}{4} \frac{1+c_V}{\sqrt{1+c_A}} \bar{K}_\mu^* \vec{\tau} \cdot (K \partial^\mu \vec{\pi} - \partial^\mu K \vec{\pi}) + \text{H.c.}, \\
\mathcal{L}_{K^* K \eta} &= i \frac{ag}{\sqrt{6}} \frac{1+c_V}{\sqrt{(1+c_A)(1+\frac{2}{3}c_A)}} \bar{K}_\mu^* (K \partial^\mu \eta - \partial^\mu K \eta) + \text{H.c.}, \\
\mathcal{L}_{\rho\rho\rho} &= g \partial_\mu \vec{\rho}_\nu \cdot (\vec{\rho}^\mu \times \vec{\rho}^\nu), \\
\mathcal{L}_{\rho K^* K^*} &= i \frac{g}{2} [(\partial_\mu \bar{K}^{*\nu} \vec{\tau} K_\nu^* - \bar{K}^{*\nu} \vec{\tau} \partial_\mu K_\nu^*) \cdot \vec{\rho}^\mu + (\bar{K}^{*\nu} \vec{\tau} \cdot \partial_\mu \vec{\rho}_\nu - \partial_\mu \bar{K}^{*\nu} \vec{\tau} \cdot \vec{\rho}_\nu) K^{*\mu} \\
&\quad + \bar{K}^{*\mu} (\vec{\tau} \cdot \vec{\rho}^\nu \partial_\mu K_\nu^* - \vec{\tau} \cdot \partial_\mu \vec{\rho}^\nu K_\nu^*)], \\
\mathcal{L}_{\omega K^* K^*} &= i \frac{g}{2} [(\partial_\mu \bar{K}^{*\nu} K_\nu^* - \bar{K}^{*\nu} \partial_\mu K_\nu^*) \omega^\mu + (\bar{K}^{*\nu} \partial_\mu \omega_\nu - \partial_\mu \bar{K}^{*\nu} \omega_\nu) K^{*\mu} \\
&\quad + \bar{K}^{*\mu} (\omega^\nu \partial_\mu K_\nu^* - \partial_\mu \omega^\nu K_\nu^*)], \\
\mathcal{L}_{\rho K^* K \eta} &= \frac{ag^2}{2\sqrt{6}} \frac{c_V}{\sqrt{(1+c_A)(1+\frac{2}{3}c_A)}} (\bar{K} \vec{\tau} K_\mu^* \cdot \vec{\rho}^\mu \eta + \bar{K}_\mu^* \vec{\tau} K \cdot \vec{\rho}^\mu \eta), \\
\mathcal{L}_{\omega K^* K \eta} &= \frac{ag^2}{2\sqrt{6}} \frac{c_V}{\sqrt{(1+c_A)(1+\frac{2}{3}c_A)}} (\bar{K} K_\mu^* \omega^\mu \eta + \bar{K}_\mu^* K \omega^\mu \eta), \\
\mathcal{L}_{\pi\eta KK} &= \frac{1}{3\sqrt{6}f_\pi^2} \frac{1}{(1+c_A)\sqrt{1+\frac{2}{3}c_A}} \left[\left(1 + \frac{3}{2}c_A\right) (\bar{K} \vec{\tau} \partial_\mu K \cdot \partial^\mu \vec{\pi} \eta + \partial_\mu \bar{K} \vec{\tau} K \cdot \partial^\mu \vec{\pi} \eta) \right. \\
&\quad + \bar{K} \vec{\tau} \partial_\mu K \cdot \vec{\pi} \partial^\mu \eta + \partial_\mu \bar{K} \vec{\tau} K \cdot \vec{\pi} \partial^\mu \eta - (2+3c_A) \bar{K} \vec{\tau} K \cdot \partial_\mu \vec{\pi} \partial^\mu \eta \\
&\quad \left. - 2\partial_\mu \bar{K} \vec{\tau} \partial^\mu K \cdot \vec{\pi} \eta + m_\pi^2 \bar{K} \vec{\tau} K \cdot \vec{\pi} \eta \right], \\
\mathcal{L}_{\rho\rho\eta} &= \frac{g_{\rho\rho\eta}}{\sqrt{6}} \frac{1}{\sqrt{1+\frac{2}{3}c_A}} \epsilon^{\mu\nu\lambda\sigma} \partial_\mu \vec{\rho}_\nu \cdot \partial_\lambda \vec{\rho}_\sigma \eta, \\
\mathcal{L}_{\omega\omega\eta} &= \frac{g_{\omega\omega\eta}}{\sqrt{6}} \frac{1}{\sqrt{1+\frac{2}{3}c_A}} \epsilon^{\mu\nu\lambda\sigma} \partial_\mu \omega_\nu \partial_\lambda \omega_\sigma \eta, \\
\mathcal{L}_{\rho\omega\pi} &= g_{\rho\omega\pi} \epsilon^{\alpha\beta\lambda\sigma} \partial_\mu \vec{\rho}_\nu \partial_\lambda \omega_\sigma \cdot \vec{\pi}, \\
\mathcal{L}_{\rho K^* K} &= \frac{g_{\rho K^* K}}{2} \frac{1}{\sqrt{1+c_A}} \epsilon^{\mu\nu\lambda\sigma} (\bar{K} \partial_\mu \vec{\rho}_\nu \cdot \vec{\tau} \partial_\lambda K_\sigma^* + \partial_\mu \vec{\rho}_\nu \cdot \partial_\lambda \bar{K}_\sigma^* \vec{\tau} K), \\
\mathcal{L}_{\omega K^* K} &= \frac{g_{\omega K^* K}}{2} \frac{1}{\sqrt{1+c_A}} \epsilon^{\mu\nu\lambda\sigma} \partial_\mu \omega_\nu (\bar{K} \partial_\lambda K_\sigma^* + \partial_\lambda \bar{K}_\sigma^* K), \\
\mathcal{L}_{K^* K^* \pi} &= \frac{g_{K^* K^* \pi}}{2} (1+2c_{wz}) \epsilon^{\mu\nu\lambda\sigma} \partial_\mu \bar{K}_\nu^* \vec{\tau} \partial_\lambda K_\sigma^* \cdot \vec{\pi}, \\
\mathcal{L}_{K^* K^* \eta} &= \frac{2g_{K^* K^* \eta}}{\sqrt{6}} \frac{c_{wz}}{\sqrt{1+\frac{2}{3}c_A}} \epsilon^{\mu\nu\lambda\sigma} \partial_\mu \bar{K}_\nu^* \partial_\lambda K_\sigma^* \eta.
\end{aligned} \tag{15}$$

In the above, $\vec{\tau}$ are Pauli matrices for isospin; and $\vec{\pi}$ and $\vec{\rho}$ denote the pion and rho meson isospin triplet, respectively; and $K = (K^+, K^0)^T$ and $K^* = (K^{*+}, K^{*0})^T$ denote the pseudoscalar and vector strange meson isospin doublet, respectively.

For the parameters in the interaction Lagrangians given in Eq.(15), we choose $a = 2$ to recover the vector dominance model and the KSFR relation. Using the empirical value $f_\pi = 92.4$ MeV for pion decay constant, $m_\rho = 776$ MeV for rho meson mass, and $m_{K^*} = 892$ MeV for K^* mass, the KSFR relation (Eq.(12)) then gives a universal vector coupling constant of $g = 5.94$ and the parameter $c_V = 0.32$. We note that a slightly larger value of $c_V = 0.36$ was obtained in Ref.[8] by fitting the empirical phi meson mass $m_\phi = 1020$ MeV. Since only the K^* is needed in present study, we choose to have the correct K^* instead phi meson mass. From Eq.(11), the parameter $c_A = 0.49$ is obtained from the empirical kaon decay constant $f_K = 1.22f_\pi$.

It is interesting to know that above parameters lead to a width $\Gamma_\rho = g^2(m_\rho^2 - 4m_\pi^2)^{3/2}/(48\pi m_\rho^2) \sim 147$ MeV for rho meson decay to two pions and a width $\Gamma_{K^*} = [g^2(1 + c_V^2)/(1 + c_A)]\{[m_{K^*}^2 - (m_K + m_\pi)^2][m_{K^*}^2 - (m_K - m_\pi)^2]\}^{3/2}/(16\pi m_{K^*}^5) \sim 49$ MeV for K^* decay to $K\pi$, which are close to the empirical values of $\Gamma_\rho = 150$ MeV and $\Gamma_{K^*} = 51$ MeV.

For the anomalous coupling constants g_{VVP} , they are related to the universal vector coupling g and pseudoscalar decay constant by [10],

$$g_{VVP} = \frac{3g^2}{8\pi^2 f_P}, \quad P = \pi, \eta, K \quad (16)$$

and from the ratio between experimental decay widths of $K^{*0} \rightarrow K^0\gamma$ and $K^{*\pm} \rightarrow K^\pm\gamma$, the parameter $c_{wz} = -0.1$ has been determined [14].

IV. ETA ABSORPTION BY MESONS

Since the temperature of the hot hadronic matter produced at RHIC is above $T = 125$ MeV, it consists of not only the lightest π mesons but also heavier ρ and ω mesons as well as the strange mesons K and K^* . Eta mesons can thus be absorbed by all these mesons.

A. Born diagrams

Diagrams for these reactions are shown in Fig. 1 for η absorption by π to the final states of $K\bar{K}$, $K\bar{K}^*(\bar{K}K^*)$, $K^*\bar{K}^*$, $\rho\omega$, and $\pi\rho$; in Fig. 2 for η absorption by ρ meson to the final states $K\bar{K}$, $K\bar{K}^*(\bar{K}K^*)$, $K^*\bar{K}^*$, $\rho\rho$, $\pi\omega$, and $\pi\pi$; in Fig. 3 for η absorption by ω meson to the final states $K\bar{K}$, $K\bar{K}^*$, $K^*\bar{K}^*$, and $\pi\rho$; and in Figs. 4 and 5 for η absorption by K and K^* to the final states of πK , πK^* , ρK , ρK^* , ωK , and ωK^* .

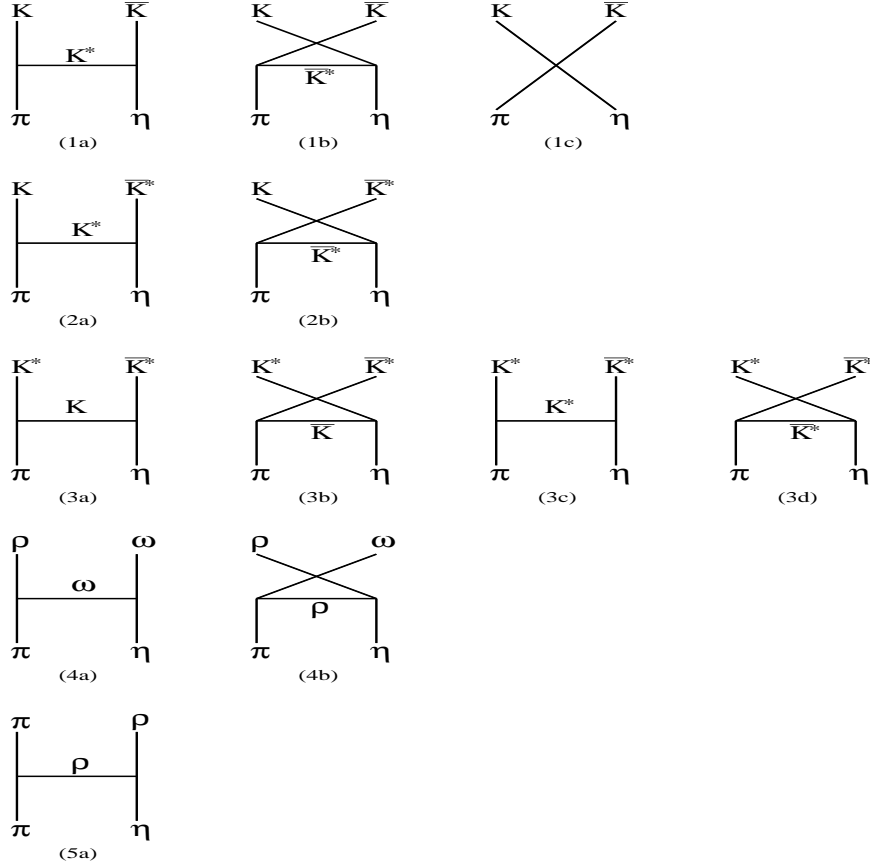


FIG. 1: Diagrams for η absorption by π meson.

Using the interaction Lagrangian densities given in Section III, we have derived the amplitudes for all tree-level diagrams shown in Figs. 1-5. In general, the amplitude for a process n is given by

$$\mathcal{M}_n = A \left(\sum_i \mathcal{M}_{ni}^{\lambda_k \dots \lambda_l} \right) \epsilon_{k\lambda_k} \dots \epsilon_{l\lambda_l}, \quad (17)$$

where i runs through all the subprocesses in each reaction, and $\epsilon_{j\lambda_j}$ denotes the polarization vector of external vector meson j . The factor A is either a matrix element τ_{ij}^a of the Pauli

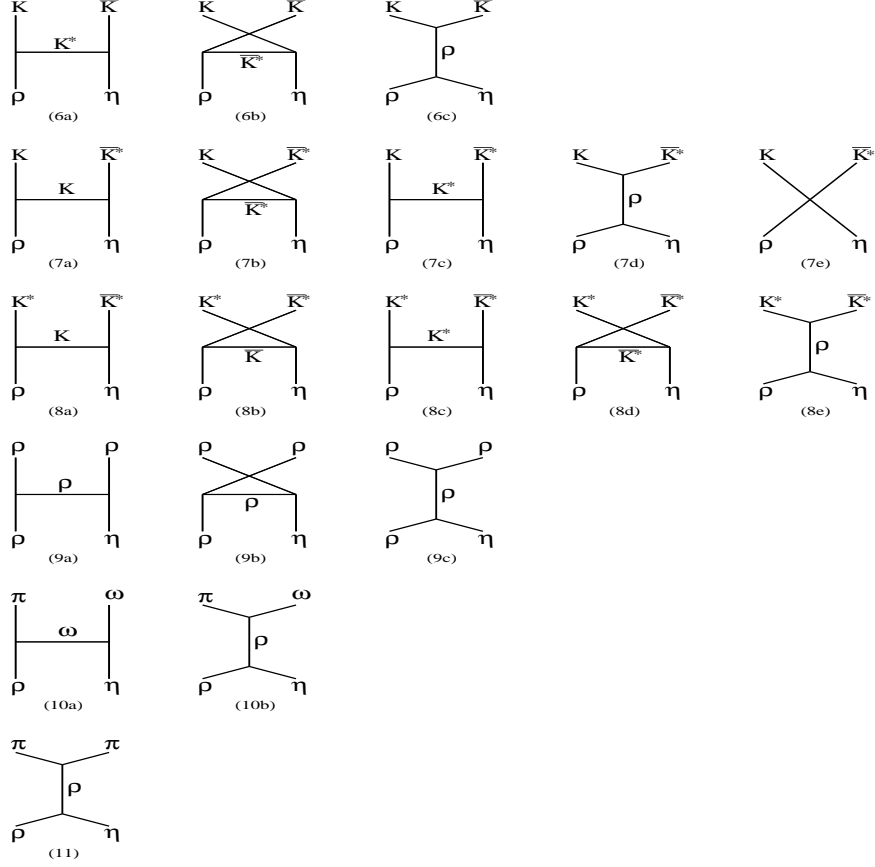


FIG. 2: Diagrams for η absorption by ρ meson.

matrices or the kronecker delta δ_{ab} or the antisymmetric tensor $i\epsilon_{abc}$. It takes into account the isospin states of the particles in a reaction, with a , b , and c denoting those of isospin triplet π and ρ meson, and i and j those of isospin doublet K and K^* . Explicit expressions for these amplitudes are given in Appendix A for η absorption by π meson, Appendix B for η absorption by ρ meson, Appendix C for η absorption by ω meson, Appendix D for η absorption by K meson, and Appendix E for η absorption by K^* meson.

B. form factors

To obtain the full amplitudes for these reactions, one needs in principle to carry out a coupled-channel calculation in order to avoid the violation of unitarity. Such an approach is, however, beyond the scope of present work. To prevent the artificial growth of the tree-level amplitudes with the energy, we introduce instead form factors at interaction vertices

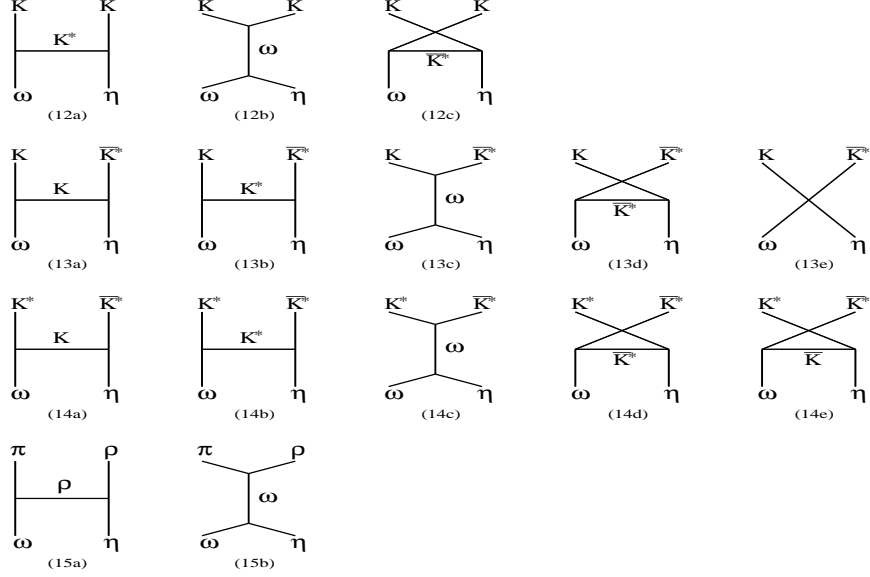


FIG. 3: Diagrams for η absorption by ω meson.

and treat their cutoff parameters as parameters. Specifically, the form factors are taken to have the same forms as used previously in studying J/ψ absorption [16, 17] and charmed meson scattering [18] by mesons, charmed meson production from photon- and proton-proton reactions [19], pentaquark baryon production from photon- and hadron-proton reactions [20], and strangeness-exchange reactions between mesons and baryons [21]. For three-point vertices, i.e., $\rho\pi\pi$, ρKK , ωKK , $K^*K\pi$, $K^*K\eta$, $\rho\rho\rho$, ρK^*K^* , ωK^*K^* , $\rho\omega\pi$, $\rho\rho\eta$, $\omega\omega\eta$, ρK^*K , ωK^*K , $K^*K^*\pi$, and $K^*K^*\eta$ in the t - and u -channel processes, the form factors are taken to have the form

$$F_3(\mathbf{q}) = \frac{\Lambda^2}{\Lambda^2 + \mathbf{q}^2}, \quad (18)$$

where \mathbf{q}^2 , taken in the center of mass, is the squared three momentum transfer. For four-point contact vertices, i.e., $\rho K^*K\eta$, $\omega K^*K\eta$, and $\pi\eta KK$, they are taken to have the form

$$F_4 = \left(\frac{\Lambda_1^2}{\Lambda_1^2 + \langle \mathbf{q}^2 \rangle} \right) \left(\frac{\Lambda_2^2}{\Lambda_2^2 + \langle \mathbf{q}^2 \rangle} \right), \quad (19)$$

where Λ_1 and Λ_2 are two different cutoff parameters at the three-point vertices present in the processes with the same initial and final particles, and $\langle \mathbf{q}^2 \rangle$ is the average value of the two squared three momenta at the three-point vertices.

For three-point vertices in s -channel processes, we introduce, however, a covariant form

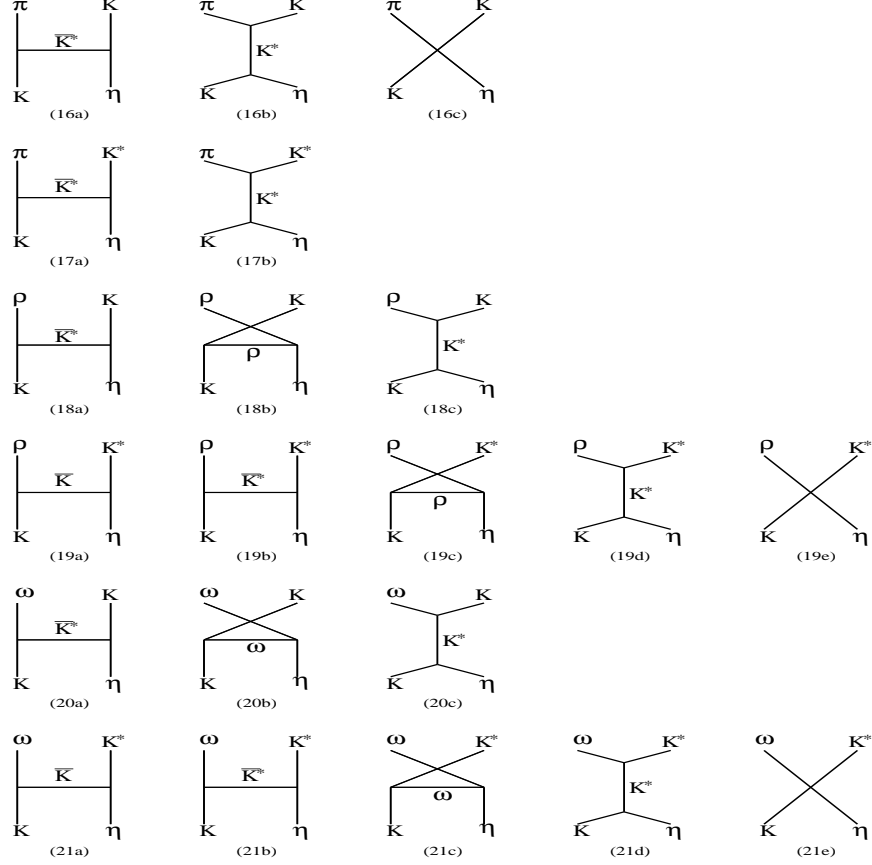


FIG. 4: Diagrams for η absorption by K meson.

factor, i.e.,

$$F'_3(s) = \frac{\Lambda^2 + m^2}{\Lambda^2 + s}, \quad (20)$$

where s is the square of the center-of-mass energy and m is the mass of the intermediate-state particle. This form factor ensures that it would not affect the predicted decay widths of ρ and K^* , which are close to the empirical ones, as $s = m^2$ in these processes. We note that unrealistic large cross sections for s -channel processes at high energies can also be prevented by taking into account the vacuum widths for all channels that are open at a given s as in Ref.[8] on phi meson interactions in hot hadronic matter.

As in previous studies on hadronic reactions, we use $\Lambda = 1$ GeV in calculating the cross sections for eta absorption by mesons. Since the value for Λ might depend on the reactions, we also study how our results are affected by changes in its value.

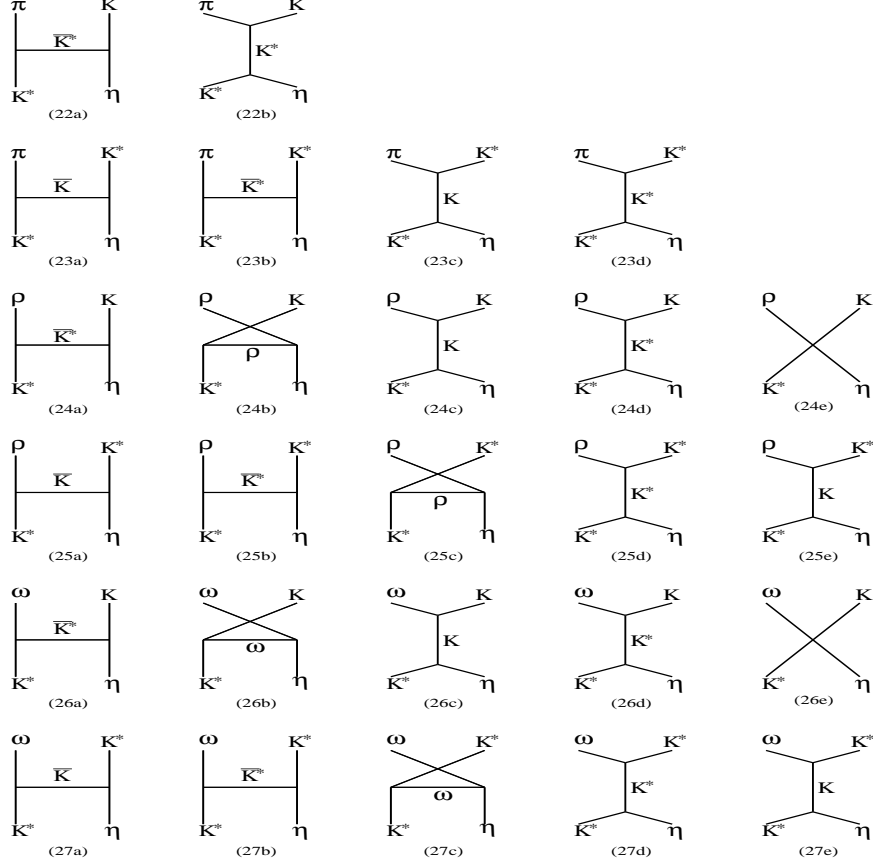


FIG. 5: Diagrams for η absorption by K^* meson.

C. cross sections for eta absorption by mesons

The isospin- and spin-averaged differential cross sections for above reactions are given by

$$\frac{d\sigma_n}{dt} = \frac{1}{64\pi s p_i^2 N_I N_S} \overline{|\mathcal{M}_n|^2}, \quad (21)$$

where $\overline{|\mathcal{M}_n|^2}$ denotes the squared amplitude obtained from summing over the isospins and spins of both initial and final particles, and can be evaluated using the software package FORM [22]. The factors $N_I = (2I_1 + 1)(2I_2 + 1)$ and $N_S = (2S_1 + 1)(2S_2 + 1)$ in the denominator are due to averaging over the isospins I_1 and I_2 as well as the spins S_1 and S_2 of initial particles, while p_i is their 3-momentum in the center-of-mass frame.

Integrating the four momentum transfer t leads to the following total cross sections:

$$\sigma_n = \frac{1}{N_I N_S} \frac{p_f}{p_i} |M_n|^2, \quad (22)$$

where p_f is the 3-momentum of final particles in their center-of-mass frame and $|M_n|^2$ is related to $|\overline{\mathcal{M}}_n|^2$ in Eq.(21) by

$$|M_n|^2 = \frac{1}{64\pi^2 s} \int d\Omega |\overline{\mathcal{M}}_n|^2 F^4, \quad (23)$$

with F denoting the appropriate form factors at interaction vertices.

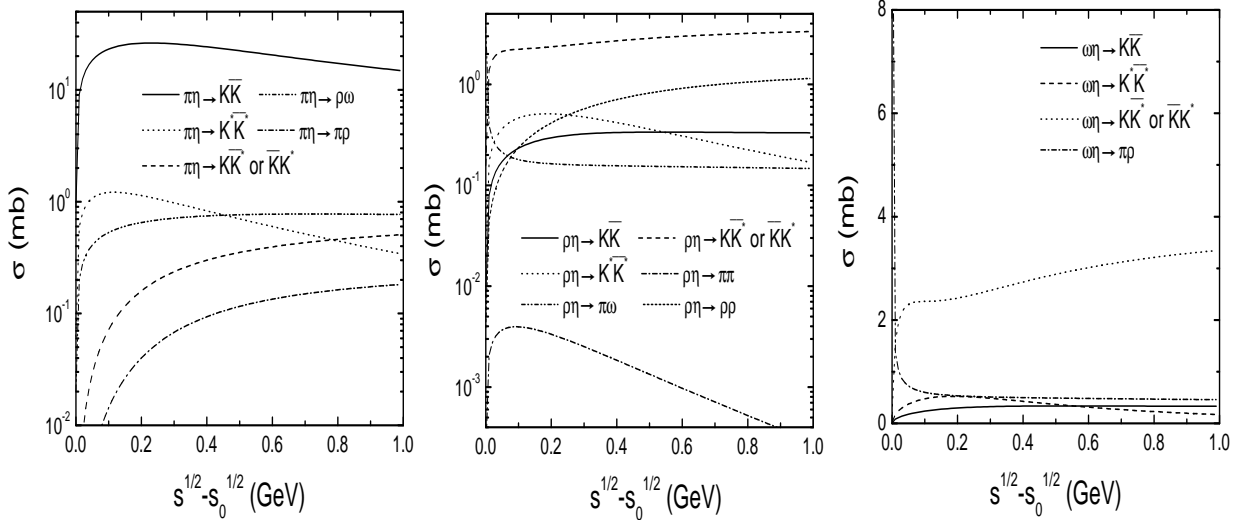


FIG. 6: Cross sections for eta absorption by π (left panel), ρ (middle panel), and ω (right panel) mesons as functions of total center-of-mass energy $s^{1/2}$ above the threshold $s_0^{1/2}$ of a reaction.

In Figs. 6 and 7, we show, respectively, the cross sections for η absorption by π , ρ , and ω mesons and by K and K^* as functions of total center-of-mass energy $s^{1/2}$ above the threshold $s_0^{1/2}$ of a reaction. Aside near the threshold of a reaction, where the cross section can be very large or small depending on whether the reaction is exothermic or endothermic, most cross sections are less than 1 mb, except the reactions $\rho\eta \rightarrow K\bar{K}^*(\bar{K}K^*)$, $\omega\eta \rightarrow K\bar{K}^*(\bar{K}K^*)$, $K^*\eta \rightarrow \rho K$, and $K^*\eta \rightarrow \omega K$, which are a few mb, and the reactions $\pi\eta \rightarrow K\bar{K}$ and $K\eta \rightarrow \pi K$, which are more than 10 mb. The large cross sections for the reactions $\pi\eta \rightarrow K\bar{K}$ and $K\eta \rightarrow \pi K$ are due to the presence of the $\pi\eta K\bar{K}$ contact interaction in their amplitudes. Values of the cross sections depend, however, on the value of the cutoff parameter in the form factors. We find that increasing the value of Λ to 2 GeV increases the cross sections by about a factor of two, but decreasing its value to 0.5 GeV reduces the cross sections by about a factor of four.

TABLE I: Values of parameters a , b , c , d , and e in Eq.(24) for parameterizing the matrix elements defined in Eq.(23).

Reactions	a	b	c	d	e
$\pi\eta \rightarrow K\bar{K}$	16.047	-468.921	-3.867	598.598	-3.215
$\pi\eta \rightarrow K\bar{K}^*(\bar{K}K^*)$	5.813	-4.232	-0.136	-1.580	-5.357
$\pi\eta \rightarrow K^*\bar{K}^*$	0.115	7.261	-13.200	8.468	-4.530
$\pi\eta \rightarrow \rho\omega$	1.539	2.577	-1.513	0.555	-15.636
$\pi\eta \rightarrow \pi\rho$	0.721	-7.012	-3.948	6.293	-4.323
$\rho\eta \rightarrow K\bar{K}$	2.706	-7.532	-5.657	4.827	-4.857
$\rho\eta \rightarrow K\bar{K}^*(\bar{K}K^*)$	36.139	20.087	-18.884	-17.458	-2.338
$\rho\eta \rightarrow K^*\bar{K}^*$	0.181	-4.174	-19.494	13.793	-4.941
$\rho\eta \rightarrow \rho\rho$	14.265	-2.296	-2.812	-10.394	-2.812
$\rho\eta \rightarrow \pi\pi$	0.001	-0.529	-8.081	0.529	-7.476
$\rho\eta \rightarrow \pi\omega$	2.007	-0.699	-5.410	-0.657	0.228
$\omega\eta \rightarrow K\bar{K}$	1.863	-0.948	-6.925	-0.878	0.056
$\omega\eta \rightarrow K\bar{K}^*(\bar{K}K^*)$	12.179	7.285	-19.514	-5.766	-2.153
$\omega\eta \rightarrow K^*\bar{K}^*$	0.060	-1.434	-19.684	4.669	-4.948
$\omega\eta \rightarrow \pi\rho$	7.784	-0.675	-5.356	-6.369	0.0317
$K\eta \rightarrow \pi K$	-33.196	78.965	-0.460	-15.275	-1.373
$K\eta \rightarrow \pi K^*$	0.00425	-18.683	-5.715	18.688	-5.511
$K\eta \rightarrow \rho K$	6.819	-5.863	-0.871	-0.955	1.118
$K\eta \rightarrow \rho K^*$	0.288	-0.413	-15.160	1.593	-5.047
$K\eta \rightarrow \omega K$	3.124	-2.091	-0.936	-1.032	0.556
$K\eta \rightarrow \omega K^*$	-0.389	-0.322	-1.785	1.182	-0.625
$K^*\eta \rightarrow \pi K$	2.078	0	-	-2.077	-2.998
$K^*\eta \rightarrow \pi K^*$	0.078	9.298	-4.638	0.514	-36.521
$K^*\eta \rightarrow \rho K$	34.849	10.952	-15.036	-16.308	-2.838
$K^*\eta \rightarrow \rho K^*$	2.999	-1.694	-27.299	1.181	-5.701
$K^*\eta \rightarrow \omega K$	11.591	3.936	-15.140	-5.276	-2.807
$K^*\eta \rightarrow \omega K^*$	0.966	-0.522	-27.134	0.409	-5.647

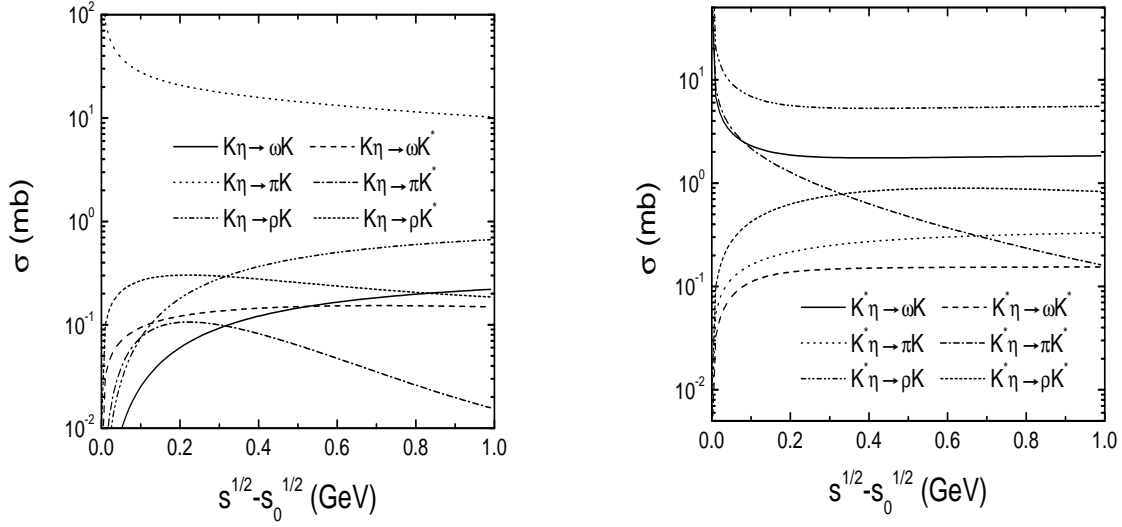


FIG. 7: Cross sections for eta absorption by K (left panel) and K^* (right panel) mesons as functions of total center-of-mass energy $s^{1/2}$ above the threshold $s_0^{1/2}$ of a reaction.

The results shown in Figs. 6 and 7 can be conveniently reproduced by parameterizing the squared matrix elements shown in Eq.(23) according to

$$|M_n|^2 = a + b \left(\frac{\sqrt{s}}{\sqrt{s_0}} \right)^c + d \left(\frac{\sqrt{s}}{\sqrt{s_0}} \right)^e \text{ mb.} \quad (24)$$

The dimensionless parameters a , b , c , d , and e for the different reactions considered in present study are given in Table I.

V. ETA PRODUCTION IN RELATIVISTIC HEAVY ION COLLISIONS

In this section, we study the effect of eta absorption reactions studied in previous sections on the time evolution of its abundance in heavy ion collisions at RHIC. We describe the collision dynamics in a schematic hydrodynamic model and assume that the hadronic matter is in thermal equilibrium throughout the collision. Furthermore, we assume that pions, rho mesons, omega mesons, and kaons as well as their resonances are in chemical equilibrium during the collision because of their larger interaction cross sections. For eta mesons, we consider two scenarios for their abundance in the beginning of the hadronic stage after hadronization of the quark-gluon plasma, i.e., they are either taken to be in chemical equilibrium with other hadrons or completely absent. Their abundance during the

evolution of the subsequent hadronic matter is then described by a kinetic model that takes into account their absorption and regeneration. We also compare the final eta number in the two scenarios with that from assuming that eta mesons remain in chemical equilibrium throughout the evolution of the hadronic matter.

A. rate equation

The density n_η of eta mesons changes in time according to the following rate equation [23]:

$$\partial_\mu(n_\eta u^\mu) = \Psi, \quad (25)$$

where $u^\mu = \gamma(1, \mathbf{v})$ is the four velocity of the hadronic matter fluid element of velocity \mathbf{v} and γ denotes the Lorentz factor. The source term Ψ is given by

$$\Psi = - \sum_{a,b,c} \langle \sigma_{a\eta \rightarrow bc} v \rangle n_\eta n_a + \sum_{a,b,c} \langle \sigma_{bc \rightarrow a\eta} v \rangle n_b n_c, \quad (26)$$

where n_a , n_b , and n_c are densities of meson types a , b , and c , respectively. The thermal averaged eta absorption and production cross sections are denoted by $\langle \sigma_{a\eta \rightarrow bc} v \rangle$ and $\langle \sigma_{bc \rightarrow a\eta} v \rangle$, respectively, with v the relative velocity of initial two interacting particles. The thermal averaged eta production cross sections are related to those of eta absorption cross sections by

$$\langle \sigma_{a\eta \rightarrow bc} v \rangle n_a^{\text{eq}} n_\eta^{\text{eq}} = \langle \sigma_{bc \rightarrow a\eta} v \rangle n_b^{\text{eq}} n_c^{\text{eq}}, \quad (27)$$

where n^{eq} denotes the equilibrium density, i.e.,

$$n^{\text{eq}} = \frac{dm^2 T}{2\pi^2} K_2(m/T). \quad (28)$$

In the above, d and m are the degeneracy and mass of a hadron, T is the temperature of the hadronic matter, and K_2 is the modified Bessel function of the second kind. Using the above relation, the rate equation can be written as

$$\partial_\mu(n_\eta u^\mu) = - \sum_{a,b,c} \langle \sigma_{a\eta \rightarrow bc} v \rangle n_a^{\text{eq}} (n_\eta - n_\eta^{\text{eq}}). \quad (29)$$

B. thermal averaged eta absorption cross sections

With particle momenta in the hadronic matter approximated by the Boltzmann distributions, the thermal averaged cross sections can be expressed as [23]

$$\langle\sigma v\rangle = [4\alpha_1^2 K_2(\alpha_1)\alpha_2^2 K_2(\alpha_2)]^{-1} \times \int_{z_0}^{\infty} dz [z^2 - (\alpha_1 + \alpha_2)^2][z^2 - (\alpha_1 - \alpha_2)^2] K_1(z) \sigma(s = z^2 T^2), \quad (30)$$

with $\alpha_i = m_i/T$, $z_0 = \max(\alpha_1 + \alpha_2, \alpha_3 + \alpha_4)$, and K_1 being the modified Bessel function of the first kind.

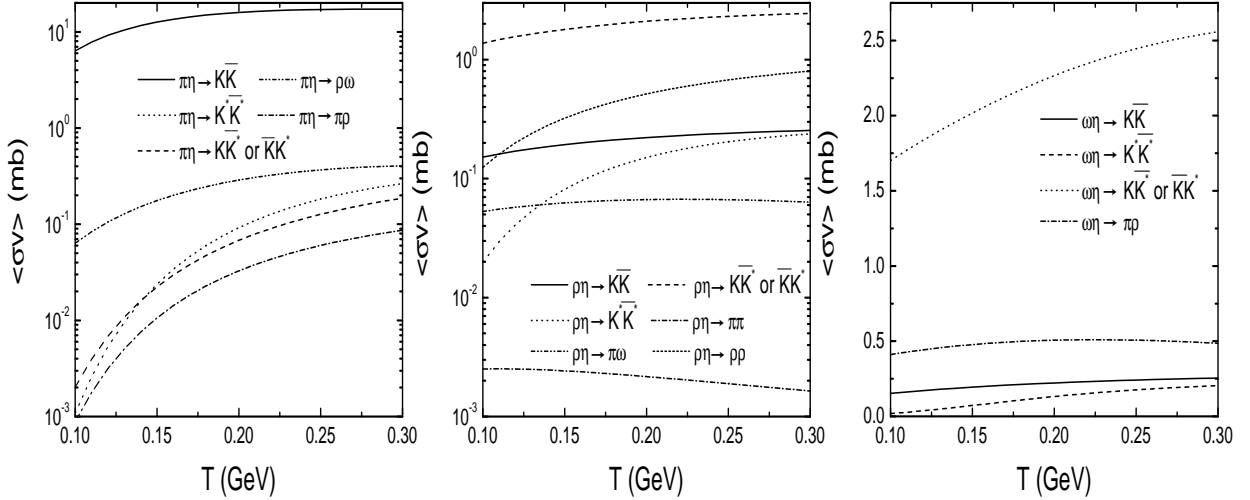


FIG. 8: Thermal averaged η absorption cross sections by pion (left panel), rho (middle panel) and omega (right panel) mesons as functions of temperature.

The resulting temperature dependence of $\langle\sigma v\rangle$ is shown in Fig. 8 for the reactions of $\pi\eta$, $\rho\eta$, and $\omega\eta$ and in Fig. 9 for the reactions of $K\eta$ and $K^*\eta$. It is seen that the thermal averaged cross sections for most reactions increase with increasing temperature. As for cross sections, the reactions $\pi\eta \rightarrow K\bar{K}$ and $K\eta \rightarrow \pi K$ have largest thermal averaged cross sections.

C. collision dynamics at RHIC

Since the particle distribution in central heavy ion collisions at RHIC is approximately uniform in midrapidity and the geometry of the collision is cylindrically symmetric, it is

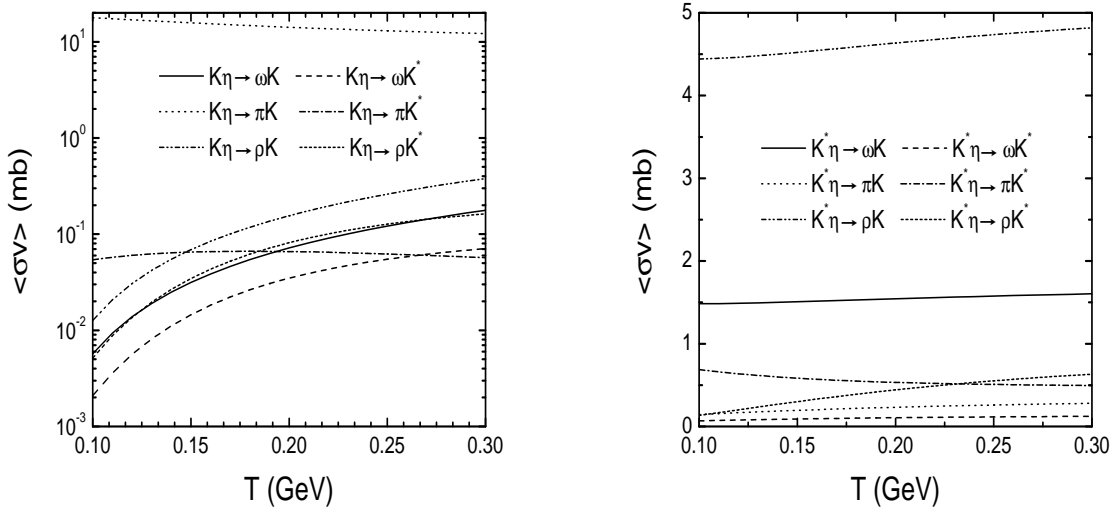


FIG. 9: Thermal averaged η absorption cross sections by K (left panel) and K^* (right panel) as functions of temperature.

convenient to use the cylindrical coordinates r , φ , τ , and η with the latter given by

$$\tau = \sqrt{t^2 - z^2}, \quad \eta = \frac{1}{2} \ln \frac{t+z}{t-z}. \quad (31)$$

Assuming longitudinal boost invariance and allowing for radial transverse expansion, then one has $u^\eta = u^\varphi = 0$. For uniform density distribution in the transverse plane, averaging over the radial coordinate gives

$$\frac{1}{\tau R^2(\tau)} \frac{\partial}{\partial \tau} (\tau R^2(\tau) n_\eta \langle u^\tau \rangle) = - \sum_{a,b,c} \langle \sigma_{\eta a \rightarrow bc} v \rangle n_a^{eq} (n_\eta - n_\eta^{eq}) \quad (32)$$

In the above, $R(\tau)$ is the transverse radius of the system and $\langle u^\tau \rangle$ is the averaged τ component of the four velocity and is given by

$$\langle u^\tau \rangle = \frac{2}{R^2(\tau)} \int_0^{R(\tau)} dr r u^\tau(r). \quad (33)$$

At midrapidity, the four velocity of hadronic fluid element u^μ can be expressed in terms of the radial flow velocity β_r as

$$u^\tau = \gamma_r = \frac{1}{\sqrt{1 - \beta_r^2}}. \quad (34)$$

With the usual ansatz for the radial velocity, i.e.,

$$\beta_r(\tau, r) = \frac{dR}{d\tau} \left(\frac{r}{R} \right), \quad (35)$$

we have

$$\langle u^\tau \rangle = \int_0^1 dy \frac{1}{\sqrt{1 - (dR/d\tau)^2} y}. \quad (36)$$

To determine the time evolution of the transverse radius of the fireball, we follow the model used in Ref.[24]. Since we are interested in the time evolution of the eta abundance during the hadronic phase of the collision, we start from the end of the mixed phase τ_H and write

$$R(\tau) = R_H + v_H(\tau - \tau_H) + \frac{a}{2}(\tau - \tau_H)^2. \quad (37)$$

In the above, $R_H \approx 9$ fm and $v_H \approx 0.4c$ are, respectively, the transverse radius and flow velocity of the fireball at $\tau_H = 7.5$ fm/ c , while $a = 0.02c^2/\text{fm}$ is the acceleration in the transverse expansion. Values of these parameters are determined from fitting the measured transverse energy $\simeq 788$ GeV as well as the extracted freeze out temperature $T_F = 125$ MeV and transverse flow velocity $\simeq 0.65c$ of midrapidity hadrons in central Au+Au collisions at $\sqrt{s_{NN}} = 200$ GeV. Assuming that the hadronic matter expands isentropically, the time dependence of the temperature of the fireball obtained in Ref.[24] can be parameterized as

$$T(\tau) = T_C - (T_H - T_F) \left(\frac{\tau - \tau_H}{\tau_F - \tau_H} \right)^{0.8}, \quad (38)$$

where T_H is the temperature of the hadronic matter at the end of the mixed phase and is thus the same as the critical temperature T_C for the quark-gluon plasma to hadronic matter transition. As in Ref.[24], we take $T_H = T_C = 175$ MeV. The freeze out temperature $T_F = 125$ MeV then leads to a freeze out time $\tau_F \approx 17.3$ fm/ c .

D. time evolution of the eta abundance

To study how the eta meson abundance evolves in time, we consider two scenarios for the initial eta meson number, i.e., no eta meson is present at τ_H or the eta meson is in chemical equilibrium with other hadrons at τ_H as in the statistical model [25]. In the first case, subsequent hadronic interactions increase the final eta meson number to about 30 at freeze out, as shown by the dotted line in the left panel of Fig. 10. This scenario is, however, unrealistic as we expect eta mesons to be appreciably produced during hadronization of the quark-gluon plasma. For example, in the quark coalescence model [26], the number of eta mesons produced at hadronization ranges from 12 for a small eta meson root mean square

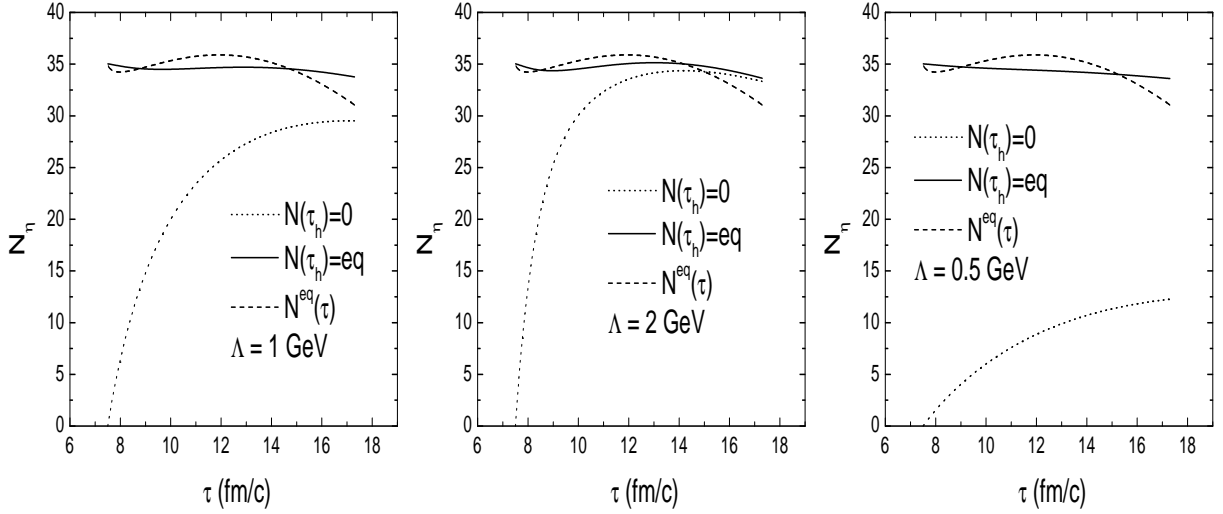


FIG. 10: Time dependence of the abundance of midrapidity η mesons in the hot hadronic gas formed from central Au+Au collisions at $\sqrt{s_{NN}} = 200$ GeV at RHIC for cutoff parameter $\Lambda = 1$ GeV (left panel), 2 GeV (middle panel), and 0.5 GeV (right panel). Solid and dotted lines correspond, respectively, to eta mesons that are chemically equilibrated or absent at the beginning of the hadronic phase, while dashed lines correspond to eta mesons that are always in chemical equilibrium.

radius of 0.5 fm to 37 for a larger radius of 1 fm. In the second scenario of equilibrated eta mesons, the initial eta meson number is $N(\tau_H) \approx 35$. Including subsequent hadronic absorption and regeneration does not change much the eta abundance, and its number at freeze out is decreased slightly to about 34 as shown by the solid line in the left panel of Fig. 10. This result is consistent with the assumption of the statistical model that hadron abundances in heavy ion collisions at RHIC are largely determined at hadronization. For comparison, we have also shown in the left panel of Fig. 10 by the dashed line results from the assumption that eta mesons are always in chemical equilibrium with other hadrons during evolution of the hadronic matter. In this case, the eta number shows a small initial increase that is followed by a decrease to about 32 at freeze out. The similarity among the final eta abundance in all three scenarios indicates that the yield of eta meson in relativistic heavy ion collisions is not very sensitive to its production mechanism. This is not surprising as the cross sections for the reactions $\pi\eta \rightarrow K\bar{K}$ and $K\eta \rightarrow \pi K$ obtained with a cutoff

parameter $\Lambda = 1$ GeV in the form factor are sufficient large, implying that eta mesons are strongly interacting and thus likely reach both thermal and chemical equilibrium in the hot hadronic matter produced at relativistic heavy ion collisions. For a larger cutoff parameter of $\Lambda = 2$ GeV in the form factor, these cross sections will be even larger, and we would expect an even more similar final eta abundance for the three scenarios, and this is indeed seen in the middle panel of Fig. 10. Even for a smaller cutoff parameter of $\Lambda = 0.5$ GeV, which leads to a much smaller cross sections for eta absorption and production, final state interactions in the hadronic matter can still keep eta mesons close to chemical equilibrium if they are initially in chemical equilibrium as shown in the right panel of Fig. 10. On the other hand, the final abundance of eta mesons will be significantly below the equilibrium value if they are initially absent in the hadronic matter, which is, however, unlikely as we have commented in the above.

VI. SUMMARY

Knowledge of eta meson interactions in hadronic matter is not only of interest in its own right but also important for extracting information on the properties of the hot dense matter formed in high energy heavy ion collisions. Since there is no empirical information on the absorption cross sections of the eta meson with pion, rho and omega mesons as well as kaon and its resonance, which are the most abundant particles in high energy heavy ion collisions, we have evaluated these cross sections based on the tree-level diagrams from the $[SU(3)_L \times SU(3)_R]_{\text{global}} \times [SU(3)_V]_{\text{local}}$ chiral Lagrangian with hidden local symmetry and including symmetry breaking effects. Using empirical hadron masses and coupling constants as well as reasonable values for the cutoff parameters in the form factors at interaction vertices, we find that although cross sections for most eta absorption reactions by mesons are less than 1 mb, the reactions $\pi\eta \rightarrow K\bar{K}$ and $K\eta \rightarrow \pi K$ are more than 10 mb. To see the effects of these reactions on the yield of eta mesons in relativistic heavy ion collisions, we have solved a kinetic equation, based on a schematic model for the dynamics of heavy ion collisions, to follow the time evolution of the abundance of eta mesons. We find that the final abundance of eta mesons at freeze out of the hadronic matter is close to chemical equilibrium, irrespective of the initial value at hadronization of the quark-gluon plasma. In particular, if eta mesons are initially in chemical equilibrium with other hadrons, their

number is not strongly affected by their subsequent interactions during the expansion of the hadronic matter.

Acknowledgments

This work was supported in part by the US National Science Foundation under Grant Nos. PHY-0098805 and PHY-0457265 and the Welch Foundation under Grant No. A-1358 (C.M.K. and W.L.) as well as by the National Science Foundation of China under Grant Nos. 10105008 and 10575071 (L.W.C.).

APPENDIX A: ETA ABSORPTION BY PION

Using subscripts 1 and 2 to denote the initial-state particles and 3 and 4 for the final-state particles in the order from left to right in all the Feynman diagrams shown in Figs. 1-5, $\epsilon_{i\mu}$ for the polarization vector of vector mesons, and also the usual Mandelstam variables $s = (p_1 + p_2)^2$, $t = (p_1 - p_3)^2$ and $u = (p_1 - p_4)^2$, the amplitudes for the absorption by mesons can be written explicitly as given below. For propagators, we do not include the width of exchanged particles as its effect is negligible due to the large threshold of the reactions. We note these expressions are obtained with $a = 2$ in the chiral Lagrangian.

1. $\pi\eta \rightarrow K\bar{K}$

The amplitude for this reaction is given by

$$\mathcal{M}_{\pi\eta \rightarrow K\bar{K}} = \tau_{ij}^a (\mathcal{M}_{1a} + \mathcal{M}_{1b} + \mathcal{M}_{1c}), \quad (\text{A1})$$

with

$$\begin{aligned} \mathcal{M}_{1a} &= \frac{g^2}{\sqrt{6}} \frac{(1 + c_V)^2}{(1 + c_A)\sqrt{1 + \frac{2}{3}c_A}} (p_1 + p_3)_\mu \frac{1}{t - m_{K^*}^2} \\ &\quad \times \left[-g^{\mu\nu} + \frac{(p_1 - p_3)^\mu (p_1 - p_3)^\nu}{m_{K^*}^2} \right] (p_2 + p_4)_\nu, \\ \mathcal{M}_{1b} &= \frac{g^2}{\sqrt{6}} \frac{(1 + c_V)^2}{(1 + c_A)\sqrt{1 + \frac{2}{3}c_A}} (p_1 + p_4)_\mu \frac{1}{u - m_{K^*}^2} \\ &\quad \times \left[-g^{\mu\nu} + \frac{(p_1 - p_4)^\mu (p_1 - p_4)^\nu}{m_{K^*}^2} \right] (p_2 + p_3)_\nu, \end{aligned}$$

$$\mathcal{M}_{1c} = \frac{1}{3\sqrt{6}f_\pi^2} \frac{1}{(1+c_A)\sqrt{1+\frac{2}{3}c_A}} \left[\left(1 + \frac{3}{2}c_A\right) (p_1 \cdot p_4 + p_1 \cdot p_3) \right. \\ \left. + p_2 \cdot p_3 + p_2 \cdot p_4 + (2+3c_A)p_1 \cdot p_2 + 2p_3 \cdot p_4 + m_\pi^2 \right]. \quad (\text{A2})$$

2. $\pi\eta \rightarrow K\bar{K}^*(\bar{K}K^*)$

The amplitude for this reaction is given by

$$\mathcal{M}_{\pi\eta \rightarrow K\bar{K}^*(\bar{K}K^*)} = \tau_{ij}^a (\mathcal{M}_{2a}^\mu + \mathcal{M}_{2b}^\mu) \epsilon_{4\mu}, \quad (\text{A3})$$

with

$$\mathcal{M}_{2a}^\mu = \frac{gg_{K^*K^*\eta}}{\sqrt{6}} \frac{(1+c_V)c_{wz}}{\sqrt{(1+c_A)(1+\frac{2}{3}c_A)}} (p_1+p_3)^\nu \\ \times \left[-g_{\nu\nu'} + \frac{(p_1-p_3)_\nu(p_1-p_3)_{\nu'}}{m_{K^*}^2} \right] \frac{1}{t-m_{K^*}^2} \epsilon^{\alpha\nu'\beta\mu} p_{4\beta} (p_2-p_4)_\alpha, \\ \mathcal{M}_{2b}^\mu = \frac{gg_{K^*K^*\pi}}{\sqrt{6}} \frac{(1+c_V)(1+2c_{wz})}{\sqrt{(1+c_A)(1+\frac{2}{3}c_A)}} \\ \times \epsilon^{\alpha\nu\beta\mu} p_{4\beta} (p_1-p_4)_\alpha \left[-g_{\nu\nu'} + \frac{(p_1-p_4)_\nu(p_1-p_4)_{\nu'}}{m_{K^*}^2} \right] \frac{1}{u-m_{K^*}^2} (p_2+p_3)^{\nu'}. \quad (\text{A4})$$

3. $\pi\eta \rightarrow K^*\bar{K}^*$

The amplitude for this reaction is given by

$$\mathcal{M}_{\pi\eta \rightarrow K^*\bar{K}^*} = \tau_{ij}^a (\mathcal{M}_{3a}^{\mu\nu} + \mathcal{M}_{3b}^{\mu\nu} + \mathcal{M}_{3c}^{\mu\nu} + \mathcal{M}_{3d}^{\mu\nu}) \epsilon_{3\mu} \epsilon_{4\nu}, \quad (\text{A5})$$

with

$$\mathcal{M}_{3a}^{\mu\nu} = \frac{g^2}{\sqrt{6}} \frac{(1+c_V)^2}{(1+c_A)\sqrt{1+\frac{2}{3}c_A}} (2p_1-p_3)^\mu \frac{1}{t-m_K^2} (2p_2-p_4)^\nu, \\ \mathcal{M}_{3b}^{\mu\nu} = \frac{g^2}{\sqrt{6}} \frac{(1+c_V)^2}{(1+c_A)\sqrt{1+\frac{2}{3}c_A}} (2p_1-p_4)^\nu \frac{1}{u-m_K^2} (2p_2-p_3)^\mu, \\ \mathcal{M}_{3c}^{\mu\nu} = \frac{g_{K^*K^*\pi} g_{K^*K^*\eta}}{\sqrt{6}} \frac{(1+2c_{wz})c_{wz}}{\sqrt{1+\frac{2}{3}c_A}} \epsilon^{\alpha\mu\beta\gamma} p_{3\alpha} (p_3-p_1)_\beta \\ \times \left[-g_{\gamma\gamma'} + \frac{(p_1-p_3)_\gamma(p_1-p_3)_{\gamma'}}{m_{K^*}^2} \right] \frac{1}{t-m_{K^*}^2} \epsilon^{\alpha'\gamma'\beta'\nu} p_{4\beta'} (p_2-p_4)_{\alpha'}, \\ \mathcal{M}_{3d}^{\mu\nu} = \frac{g_{K^*K^*\pi} g_{K^*K^*\eta}}{\sqrt{6}} \frac{(1+2c_{wz})c_{wz}}{\sqrt{1+\frac{2}{3}c_A}} \epsilon^{\alpha\gamma\beta\nu} p_{4\beta} (p_4-p_1)_\alpha$$

$$\times \left[-g_{\gamma\gamma'} + \frac{(p_1 - p_4)_\gamma (p_1 - p_4)_{\gamma'}}{m_{K^*}^2} \right] \frac{1}{u - m_{K^*}^2} \epsilon^{\alpha'\mu\beta'\gamma'} p_{3\alpha'} (p_2 - p_3)_{\beta'}. \quad (\text{A6})$$

4. $\pi\eta \rightarrow \rho\omega$

The amplitude for this reaction is given by

$$\mathcal{M}_{\pi\eta \rightarrow \rho\omega} = \delta_{ab} (\mathcal{M}_{4a}^{\mu\nu} + \mathcal{M}_{4b}^{\mu\nu}) \epsilon_{3\mu} \epsilon_{4\nu}, \quad (\text{A7})$$

with

$$\begin{aligned} \mathcal{M}_{4a}^{\mu\nu} &= \frac{g_{\rho\omega\pi} g_{\omega\omega\eta}}{\sqrt{6}} \frac{1}{\sqrt{1 + \frac{2}{3}c_A}} \epsilon^{\alpha\mu\beta\gamma} p_{3\alpha} (p_3 - p_1)_\beta \\ &\times \left[-g_{\gamma\gamma'} + \frac{(p_1 - p_3)_\gamma (p_1 - p_3)_{\gamma'}}{m_\rho^2} \right] \frac{1}{t - m_\rho^2} \epsilon^{\alpha'\gamma'\beta'\nu} p_{4\beta'} (p_2 - p_4)_{\alpha'}, \\ \mathcal{M}_{4b}^{\mu\nu} &= \frac{g_{\rho\omega\pi} g_{\rho\rho\eta}}{\sqrt{6}} \frac{1}{\sqrt{1 + \frac{2}{3}c_A}} \epsilon^{\alpha\gamma\beta\nu} p_{4\beta} (p_4 - p_1)_\alpha \\ &\times \left[-g_{\gamma\gamma'} + \frac{(p_1 - p_4)_\gamma (p_1 - p_4)_{\gamma'}}{m_\rho^2} \right] \frac{1}{u - m_\rho^2} \epsilon^{\alpha'\mu\beta'\gamma'} p_{3\alpha'} (p_2 - p_3)_{\beta'}. \end{aligned} \quad (\text{A8})$$

5. $\pi\eta \rightarrow \pi\rho$

The amplitude for this reaction is given by

$$\mathcal{M}_{\pi\eta \rightarrow \pi\rho} = i\epsilon_{abc} \mathcal{M}_5^\mu \epsilon_{4\mu}, \quad (\text{A9})$$

with

$$\begin{aligned} \mathcal{M}_5^\mu &= \frac{gg_{\rho\rho\eta}}{\sqrt{6}} \frac{1}{\sqrt{1 + \frac{2}{3}c_A}} (p_1 + p_3)^\nu \\ &\times \left[-g_{\nu\nu'} + \frac{(p_1 - p_3)_\nu (p_1 - p_3)_{\nu'}}{m_\rho^2} \right] \frac{1}{t - m_\rho^2} \epsilon^{\alpha\nu'\beta\mu} p_{4\beta} (p_2 - p_4)_\alpha. \end{aligned} \quad (\text{A10})$$

APPENDIX B: ETA ABSORPTION BY RHO MESON

1. $\rho\eta \rightarrow K\bar{K}$

The amplitude for this reaction is given by

$$\mathcal{M}_{\rho\eta \rightarrow K\bar{K}} = \tau_{ij}^a (\mathcal{M}_{6a}^\mu + \mathcal{M}_{6b}^\mu + \mathcal{M}_{6c}^\mu) \epsilon_{1\mu}, \quad (\text{B1})$$

with

$$\begin{aligned}
\mathcal{M}_{6a}^\mu &= \frac{gg_{\rho K^* K}}{\sqrt{6}} \frac{1+c_V}{(1+c_A)\sqrt{1+\frac{2}{3}c_A}} \epsilon^{\nu\mu\alpha\beta} p_{1\nu} (p_3-p_1)_\alpha \\
&\quad \times \left[-g_{\beta\beta'} + \frac{(p_1-p_3)_\beta (p_1-p_3)_{\beta'}}{m_{K^*}^2} \right] \frac{1}{t-m_{K^*}^2} (p_2+p_4)^{\beta'}, \\
\mathcal{M}_{6b}^\mu &= \frac{gg_{\rho K^* K}}{\sqrt{6}} \frac{1+c_V}{(1+c_A)\sqrt{1+\frac{2}{3}c_A}} \epsilon^{\nu\mu\alpha\beta} p_{1\nu} (p_1-p_4)_\alpha \\
&\quad \times \left[-g_{\beta\beta'} + \frac{(p_1-p_4)_\beta (p_1-p_4)_{\beta'}}{m_{K^*}^2} \right] \frac{1}{u-m_{K^*}^2} (p_2+p_3)^{\beta'}, \\
\mathcal{M}_{6c}^\mu &= \frac{gg_{\rho\rho\eta}}{2\sqrt{6}} \frac{1}{(1+c_A)\sqrt{1+\frac{2}{3}c_A}} \epsilon^{\nu\mu\alpha\beta} p_{1\nu} (p_1+p_2)_\alpha \\
&\quad \times \left[-g_{\beta\beta'} + \frac{(p_1+p_2)_\beta (p_1+p_2)_{\beta'}}{m_\rho^2} \right] \frac{1}{s-m_\rho^2} (p_4-p_3)^{\beta'}.
\end{aligned} \tag{B2}$$

2. $\rho\eta \rightarrow K\bar{K}^*(\bar{K}K^*)$

The amplitude for this reaction is given by

$$\mathcal{M}_{\rho\eta \rightarrow K\bar{K}^*(\bar{K}K^*)} = \tau_{ij}^a (\mathcal{M}_{7a}^{\mu\nu} + \mathcal{M}_{7b}^{\mu\nu} + \mathcal{M}_{7c}^{\mu\nu} + \mathcal{M}_{7d}^{\mu\nu} + \mathcal{M}_{7e}^{\mu\nu}) \epsilon_{1\mu} \epsilon_{4\nu}, \tag{B3}$$

with

$$\begin{aligned}
\mathcal{M}_{7a}^{\mu\nu} &= \frac{g^2(1+c_V)}{\sqrt{6}\sqrt{(1+c_A)^3}\sqrt{1+\frac{2}{3}c_A}} (2p_3-p_1)^\mu \frac{1}{t-m_K^2} (2p_2-p_4)^\nu, \\
\mathcal{M}_{7b}^{\mu\nu} &= \frac{g^2(1+c_V)}{\sqrt{6}\sqrt{(1+c_A)(1+\frac{2}{3}c_A)}} [(2p_4-p_1)^\mu g^{\nu\alpha} + (2p_1-p_4)^\nu g^{\mu\alpha} - (p_4+p_1)^\alpha g^{\mu\nu}] \\
&\quad \times \frac{1}{u-m_{K^*}^2} \left[-g_{\alpha\beta} + \frac{(p_1-p_4)_\alpha (p_1-p_4)_\beta}{m_{K^*}^2} \right] (p_2+p_3)^\beta, \\
\mathcal{M}_{7c}^{\mu\nu} &= \frac{g_{K^*K^*\eta}^2}{\sqrt{6}} \frac{c_{wz}}{\sqrt{(1+c_A)(1+\frac{2}{3}c_A)}} \epsilon^{\alpha\mu\beta\gamma} p_{1\alpha} (p_3-p_1)_\beta \\
&\quad \times \left[-g_{\gamma\gamma'} + \frac{(p_1-p_3)_\gamma (p_1-p_3)_{\gamma'}}{m_{K^*}^2} \right] \frac{1}{t-m_{K^*}^2} \epsilon^{\alpha'\nu\beta'\gamma'} p_{4\alpha'} (p_4-p_2)_{\beta'}, \\
\mathcal{M}_{7d}^{\mu\nu} &= -\frac{g_{\rho\rho\eta}g_{\rho K^* K}}{2\sqrt{6}} \frac{1}{\sqrt{(1+c_A)(1+\frac{2}{3}c_A)}} \epsilon^{\alpha\mu\beta\gamma} p_{1\alpha} (p_1+p_2)_\beta \\
&\quad \times \left[-g_{\gamma\gamma'} + \frac{(p_1+p_2)_\gamma (p_1+p_2)_{\gamma'}}{m_\rho^2} \right] \frac{1}{s-m_\rho^2} \epsilon^{\alpha'\nu\beta'\gamma'} p_{4\alpha'} (p_3+p_4)_{\beta'}, \\
\mathcal{M}_{7e}^{\mu\nu} &= \frac{g^2}{\sqrt{6}} \frac{c_V}{\sqrt{(1+c_A)(1+\frac{2}{3}c_A)}} g^{\mu\nu}.
\end{aligned} \tag{B4}$$

3. $\rho\eta \rightarrow K^* \bar{K}^*$

The amplitude for this reaction is given by

$$\mathcal{M}_{\rho\eta \rightarrow K^* \bar{K}^*} = \tau_{ij}^a (\mathcal{M}_{8a}^{\mu\nu\alpha} + \mathcal{M}_{8b}^{\mu\nu\alpha} + \mathcal{M}_{8c}^{\mu\nu\alpha} + \mathcal{M}_{8d}^{\mu\nu\alpha} + \mathcal{M}_{8e}^{\mu\nu\alpha}) \epsilon_{1\mu} \epsilon_{3\nu} \epsilon_{4\alpha}, \quad (\text{B5})$$

with

$$\begin{aligned} \mathcal{M}_{8a}^{\mu\nu\alpha} &= \frac{gg_{\rho K^* K}}{\sqrt{6}} \frac{1 + c_V}{(1 + c_A) \sqrt{1 + \frac{2}{3}c_A}} \epsilon^{\beta\mu\gamma\nu} p_{1\beta} p_{3\gamma} \frac{1}{t - m_K^2} (2p_2 - p_4)^\alpha, \\ \mathcal{M}_{8b}^{\mu\nu\alpha} &= \frac{gg_{\rho K^* K}}{\sqrt{6}} \frac{1 + c_V}{(1 + c_A) \sqrt{1 + \frac{2}{3}c_A}} \epsilon^{\beta\mu\gamma\alpha} p_{1\beta} p_{4\gamma} \frac{1}{u - m_K^2} (p_3 - 2p_2)^\nu, \\ \mathcal{M}_{8c}^{\mu\nu\alpha} &= \frac{gg_{K^* K^* \eta}}{\sqrt{6}} \frac{c_{wz}}{\sqrt{(1 + \frac{2}{3}c_A)}} \\ &\quad \times [(2p_1 - p_3)^\nu g^{\mu\gamma} + (2p_3 - p_1)^\mu g^{\gamma\nu} - (p_1 + p_3)^\gamma g^{\mu\nu}] \\ &\quad \times \frac{1}{t - m_{K^*}^2} \left[-g_{\gamma\gamma'} + \frac{(p_1 - p_3)_\gamma (p_1 - p_3)_{\gamma'}}{m_{K^*}^2} \right] \epsilon^{\beta\gamma'\lambda\alpha} p_{4\lambda} (p_2 - p_4)_\beta, \\ \mathcal{M}_{8d}^{\mu\nu\alpha} &= \frac{gg_{K^* K^* \eta}}{\sqrt{6}} \frac{c_{wz}}{\sqrt{(1 + \frac{2}{3}c_A)}} \\ &\quad \times [(2p_1 - p_4)^\alpha g^{\mu\gamma} + (2p_4 - p_1)^\mu g^{\gamma\alpha} - (p_1 + p_4)^\gamma g^{\mu\alpha}] \\ &\quad \times \frac{1}{u - m_{K^*}^2} \left[-g_{\gamma\gamma'} + \frac{(p_1 - p_4)_\gamma (p_1 - p_4)_{\gamma'}}{m_{K^*}^2} \right] \epsilon^{\beta\gamma'\lambda\nu} p_{3\lambda} (p_2 - p_3)_\beta, \\ \mathcal{M}_{8e}^{\mu\nu\alpha} &= \frac{gg_{\rho\eta}}{2\sqrt{6}} \frac{1}{\sqrt{(1 + \frac{2}{3}c_A)}} \\ &\quad \times [-(p_3 + 2p_4)^\nu g^{\gamma\alpha} - (p_3 - p_4)^\gamma g^{\nu\alpha} + (2p_3 + p_4)^\alpha g^{\nu\gamma}] \\ &\quad \times \frac{1}{s - m_\rho^2} \left[-g_{\gamma\gamma'} + \frac{(p_1 + p_2)_\gamma (p_1 + p_2)_{\gamma'}}{m_\rho^2} \right] \epsilon^{\beta\mu\lambda\gamma'} p_{1\beta} (p_1 + p_2)_\lambda. \end{aligned} \quad (\text{B6})$$

4. $\rho\eta \rightarrow \rho\rho$

The amplitude for this reaction is given by

$$\mathcal{M}_{\rho\eta \rightarrow \rho\rho} = i\epsilon_{abc} (\mathcal{M}_{9a}^{\mu\nu\alpha} + \mathcal{M}_{9b}^{\mu\nu\alpha} + \mathcal{M}_{9c}^{\mu\nu\alpha}) \epsilon_{1\mu} \epsilon_{3\nu} \epsilon_{4\alpha}, \quad (\text{B7})$$

with

$$\begin{aligned} \mathcal{M}_{9a}^{\mu\nu\alpha} &= \frac{gg_{\rho\eta}}{\sqrt{6}} \frac{1}{\sqrt{1 + \frac{2}{3}c_A}} \\ &\quad \times [(2p_1 - p_3)^\nu g^{\mu\gamma} + (2p_3 - p_1)^\mu g^{\gamma\nu} - (p_1 + p_3)^\gamma g^{\mu\nu}] \\ &\quad \times \frac{1}{t - m_\rho^2} \left[-g_{\gamma\gamma'} + \frac{(p_1 - p_3)_\gamma (p_1 - p_3)_{\gamma'}}{m_\rho^2} \right] \epsilon^{\beta\gamma'\lambda\alpha} p_{4\lambda} (p_2 - p_4)_\beta, \end{aligned}$$

$$\begin{aligned}
\mathcal{M}_{9b}^{\mu\nu\alpha} &= \frac{gg_{\rho\rho\eta}}{\sqrt{6}} \frac{1}{\sqrt{1 + \frac{2}{3}c_A}} \\
&\times [(2p_1 - p_4)^\alpha g^{\mu\gamma} + (2p_4 - p_1)^\mu g^{\gamma\alpha} - (p_1 + p_4)^\gamma g^{\mu\alpha}] \\
&\times \frac{1}{u - m_\rho^2} \left[-g_{\gamma\gamma'} + \frac{(p_1 - p_4)_\gamma (p_1 - p_4)_{\gamma'}}{m_\rho^2} \right] \epsilon^{\beta\gamma'\lambda\nu} p_{3\lambda} (p_2 - p_3)_\beta, \\
\mathcal{M}_{9c} &= \frac{gg_{\rho\rho\eta}}{\sqrt{6}} \frac{1}{\sqrt{1 + \frac{2}{3}c_A}} \\
&\times [-(p_3 + 2p_4)^\nu g^{\gamma\alpha} - (p_3 - p_4)^\gamma g^{\nu\alpha} + (2p_3 + p_4)^\alpha g^{\nu\gamma}] \\
&\times \frac{1}{s - m_\rho^2} \left[-g_{\gamma\gamma'} + \frac{(p_1 + p_2)_\gamma (p_1 + p_2)_{\gamma'}}{m_\rho^2} \right] \epsilon^{\beta\mu\lambda\gamma'} p_{1\beta} (p_1 + p_2)_\lambda. \tag{B8}
\end{aligned}$$

5. $\rho\eta \rightarrow \pi\omega$ and $\rho\eta \rightarrow \pi\pi$

The amplitudes $\mathcal{M}_{\rho\eta \rightarrow \pi\omega}$ for the reaction $\rho\eta \rightarrow \pi\omega$ and $\mathcal{M}_{\rho\eta \rightarrow \pi\pi}$ for the reaction $\rho\eta \rightarrow \pi\pi$ can be obtained from the amplitudes for the reaction $\pi\eta \rightarrow \rho\omega$ and $\pi\eta \rightarrow \pi\rho$ via crossing symmetry, i.e., interchanging p_1 with either $-p_3$ or $-p_4$. Explicitly, they are given by

$$\begin{aligned}
\mathcal{M}_{\rho\eta \rightarrow \pi\omega} &= \mathcal{M}_{\pi\eta \rightarrow \rho\omega}(p_1 \leftrightarrow -p_3), \\
\mathcal{M}_{\rho\eta \rightarrow \pi\pi} &= \mathcal{M}_{\pi\eta \rightarrow \pi\rho}(p_1 \leftrightarrow -p_4). \tag{B9}
\end{aligned}$$

APPENDIX C: ETA ABSORPTION BY OMEGA MESON

The amplitudes for these reactions can be obtained from corresponding ones for eta absorption by ρ^0 meson by replacing the mass of the ρ meson with that of ω meson or by the crossing symmetry via interchanging p_1 with $-p_4$, i.e.,

$$\begin{aligned}
\mathcal{M}_{\omega\eta \rightarrow K\bar{K}} &= \mathcal{M}_{\rho^0\eta \rightarrow K\bar{K}}(m_\rho \rightarrow m_\omega), \\
\mathcal{M}_{\omega\eta \rightarrow K\bar{K}^*(\bar{K}K^*)} &= \mathcal{M}_{\rho^0\eta \rightarrow K\bar{K}^*(\bar{K}K^*)}(m_\rho \rightarrow m_\omega), \\
\mathcal{M}_{\omega\eta \rightarrow K^*\bar{K}^*} &= \mathcal{M}_{\rho^0\eta \rightarrow K^*\bar{K}^*}(m_\rho \rightarrow m_\omega), \\
\mathcal{M}_{\omega\eta \rightarrow \pi\rho} &= \mathcal{M}_{\rho\eta \rightarrow \pi\omega}(p_1 \leftrightarrow -p_4). \tag{C1}
\end{aligned}$$

APPENDIX D: ETA ABSORPTION BY K MESON

The amplitudes for the final states of πK , πK^* , ρK , and ρK^* can be obtained from those for the reactions shown in Figs. 1 and 2 using the crossing symmetry. For the final states

of ωK and ωK^* , the amplitudes are related to those with final states $\rho^0 K$ and $\rho^0 K^*$ by replacing the mass of ρ meson with that of ω meson, i.e.,

$$\begin{aligned}
\mathcal{M}_{K\eta\rightarrow\pi K} &= \mathcal{M}_{\pi\eta\rightarrow K\bar{K}}(p_1 \leftrightarrow -p_3), \\
\mathcal{M}_{K\eta\rightarrow\pi K^*} &= \mathcal{M}_{\pi\eta\rightarrow K\bar{K}^*}(p_1 \leftrightarrow -p_3), \\
\mathcal{M}_{K\eta\rightarrow\rho K} &= \mathcal{M}_{\rho\eta\rightarrow K\bar{K}}(p_1 \leftrightarrow -p_3), \\
\mathcal{M}_{K\eta\rightarrow\rho K^*} &= \mathcal{M}_{\rho\eta\rightarrow K\bar{K}^*}(p_1 \leftrightarrow -p_3), \\
\mathcal{M}_{K\eta\rightarrow\omega K} &= \mathcal{M}_{K\eta\rightarrow\rho^0 K}(m_\rho \rightarrow m_\omega), \\
\mathcal{M}_{K\eta\rightarrow\omega K^*} &= \mathcal{M}_{K\eta\rightarrow\rho^0 K^*}(m_\rho \rightarrow m_\omega).
\end{aligned} \tag{D1}$$

APPENDIX E: ETA ABSORPTION BY K^* MESON

Their amplitudes can also be obtained from those for other reactions via the crossing symmetry or replacing the mass of ρ meson with that of ω meson, i.e.,

$$\begin{aligned}
\mathcal{M}_{K^*\eta\rightarrow\pi K} &= \mathcal{M}_{K\eta\rightarrow\pi K^*}(p_1 \leftrightarrow -p_3), \\
\mathcal{M}_{K^*\eta\rightarrow\pi K^*} &= \mathcal{M}_{\pi\eta\rightarrow K^*\bar{K}^*}(p_1 \leftrightarrow -p_4), \\
\mathcal{M}_{K^*\eta\rightarrow\rho K} &= \mathcal{M}_{K\eta\rightarrow\rho K^*}(p_1 \leftrightarrow -p_4), \\
\mathcal{M}_{K^*\eta\rightarrow\rho K^*} &= \mathcal{M}_{\rho\eta\rightarrow K^*\bar{K}^*}(p_1 \leftrightarrow -p_3), \\
\mathcal{M}_{K^*\eta\rightarrow\omega K} &= \mathcal{M}_{K^*\eta\rightarrow\rho^0 K}(m_\rho \rightarrow m_\omega), \\
\mathcal{M}_{K^*\eta\rightarrow\omega K^*} &= \mathcal{M}_{K^*\eta\rightarrow\rho^0 K^*}(m_\rho \rightarrow m_\omega).
\end{aligned} \tag{E1}$$

-
- [1] O. Schwalb *et al.*, Phys. Lett. B **321**, 20 (1994); F.D. Bert *et al.*, Phys. Rev. Lett. **72**, 977 (1994); R. Averbeck *et al.*, Z. Phys. A **359**, 65 (1997).
 - [2] G. Q. Li, C. M. Ko, and G. E. Brown, Phys. Rev. Lett. **75**, 4007 (1995).
 - [3] Z. W. Lin, C. M. Ko, and S. Pal, Phys. Rev. Lett. **89**, 152301 (2002).
 - [4] A. De Paoli, K. W. Cassing, U. Mosel, and C. M. Ko, Phys. Lett. B **219**, 194 (1989).
 - [5] G. Q. Li, C. M. Ko, and G. E. Brown, Nucl. Phys. A **606**, 568 (1996); G. Q. Li, C. M. Ko, G. E. Brown, and H. Sorge, *ibid.*, **611**, 539 (1996).

- [6] M. Bando, T. Kugo, S. Uehara, K. Yamawaki, and T. Yanagida, Phys. Rev. Lett. **54**, 1215 (1985).
- [7] C. Song, S. H. Lee, and C. M. Ko, Phys. Rev. C **52**, R476 (1995); C. Song, V. Koch, S. H. Lee, and C. M. Ko, Phys. Lett. B **366**, 379 (1996).
- [8] L. Alvarez-Ruso and V. Koch, Phys. Rev. C **65**, 054901 (2002).
- [9] D. Black, A. H. Fariborz, and J. Schechter, Phys. Rev. D **61**, 074030 (2000).
- [10] K. Kawarabayashi and M. Suzuki, Phys. Rev. Lett. **16**, 255 (1966); Riazuddin and Fayyazuddin, Phys. Rev. **147**, 1071 (1966).
- [11] J. Sakurai, Ann. Phys. **11**, 1 (1960).
- [12] A. Bramon, Phys. Lett. B **51**, 87 (1974).
- [13] D. E. Groom *et al.*, Particle Data Group, Eur. Phys. J. C **15**, 1 (2000).
- [14] A. Bramon, A. Grau, and G. Pancheri, Phys. Lett. B **345**, 263 (1995).
- [15] T. Fujiwara, T. Kugo, H. Terao, S. Uehara, and K. Yamawaki, Prog. Theor. Phys. **73**, 926 (1985).
- [16] Z. W. Lin and C. M. Ko, Phys. Rev. C **62**, 034903 (2000).
- [17] W. Liu, C. M. Ko, and Z. W. Lin, Phys. Rev. C **65**, 015203 (2001).
- [18] Z. W. Lin, T. G. Di, and C. M. Ko, Nucl. Phys. A **689**, 965 (2001).
- [19] W. Liu, S. H. Lee, and C. M. Ko, Nucl. Phys. A **724**, 375 (2003); W. Liu, C. M. Ko, and S. H. Lee, *ibid.* **728**, 457 (2003).
- [20] W. Liu and C. M. Ko, Phys. Rev. C **68**, 045203 (2003).
- [21] C. H. Li and C. M. Ko, Nucl. Phys. A **712**, 110 (2002).
- [22] J. Vermaseren, computer code FORM, 1989. Free version of the software is available on the Internet at <ftp://hep.itp.tuwien.ac.at/pub/Form/PC/>.
- [23] L. H. Xia and C. M. Ko, Phys. Rev. C **38**, 179 (1988); L. H. Xia, C. M. Ko, and C. T. Li, Phys. Rev. C **41**, 572 (1990); G. E. Brown, C. M. Ko, Z. G. Wu, and L. H. Xia, Phys. Rev. C **43**, 1881 (1991).
- [24] L. W. Chen, V. Greco, C. M. Ko, S. H. Lee, and W. Liu, Phys. Lett. B **601**, 34 (2004).
- [25] P. Braun-Munzinger, D. Majestra, K. Redlich, and J. Stachel, Phys. Lett. B **518**, 41 (2001).
- [26] V. Greco, C. M. Ko, and P. Lévai, Phys. Rev. Lett. **90**, 202302 (2003); Phys. Rev. C **68**, 034904 (2003).